Hierarchical Graphene/Metal Grid Structures for Stable, Flexible Transparent Conductors

Tongchuan Gao,[†] Zhiting Li,[‡] Po-shun Huang,[§] Ganesh J. Shenoy,[‡] David Parobek,[‡] Susheng Tan,[⊥] Jung-kun Lee,[§] Haitao Liu,[‡] and Paul W. Leu[*,†]

[†]Department of Industrial Engineering, [‡]Department of Chemistry, [§]Department of Mechanical Engineering & Materials Science, and [⊥]Department of Electrical and Computer Engineering & Petersen Institute of NanoScience and Engineering, University of Pittsburgh, Pittsburgh, Pennsylvania 15261, United States

ABSTRACT We report an experimental study on the fabrication and characterization of hierarchical graphene/metal grid structures for transparent conductors. The hierarchical structure allows for uniform and local current conductivity due to the graphene and exhibits low sheet resistance because the microscale silver grid serves as a conductive backbone. Our samples demonstrate 94% diffusive transmission with a sheet resistance of 0.6 Ω/sq and a direct current to optical conductivity ratio σ_{dc}/σ_{op} of 8900. The sheet resistance of the hierarchical structure may be improved by over 3 orders of magnitude and with little decrease in transmission compared with graphene. Furthermore, the graphene protects the silver grid from thermal oxidation and better maintains the sheet resistance of the structure at elevated temperature. The graphene also strengthens the adhesion of the metal grid with the substrate such that the structure is more resilient under repeated bending.

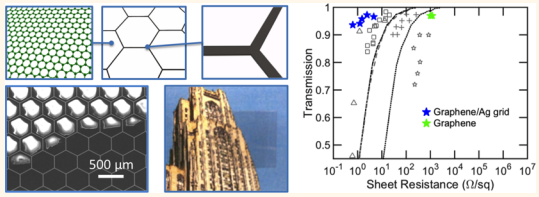

KEYWORDS: graphene · silver · hierarchical structure · transparent conductors · flexible devices

Transparent conductors are important as the top electrode for a variety of optoelectronic devices, including solar cells, light-emitting diodes, flat panel displays, and touch screens. Indium tin oxide (ITO) thin films, which can achieve a transmission of $T = 90\%$ with a sheet resistance of $R_s = 10$ Ω/sq, are the predominant transparent conductor material.[1] However, indium is a rare metal, and its price has been rising in recent years.[2] Furthermore, ITO is commercially deposited by dc magnetron sputtering, involving high-temperature processing, which makes it unsuitable for organic substrates.[3]

There has been much interest in carbon nanostructured materials, such as random carbon nanotube networks[4−7] and graphene,[8,9] as a potential substitute for ITO. However, carbon nanotubes are very expensive, and they suffer from high tube−tube resistance such that their performance has yet to exceed ITO. Graphene films (ranging from monolayer graphene to ultrathin graphite) have recently emerged as a promising transparent electrode material due to its high carrier mobility and high transparency when thin.[10,11] However, theoretical estimates of single-crystalline graphene films suggest that the highest achievable figure of merit (FoM) is $\sigma_{dc}/\sigma_{op} = 11$ or $R_s = 317$ Ω/sq at $T = 90\%$.[12] This performance is worse than even the minimum performance needs of transparent conductors in industry, which are $\sigma_{dc}/\sigma_{op} = 35$ or $R_s = 100$ Ω/sq at $T = 90\%$.[12] Experimentally fabricated graphene typically suffers from much higher sheet resistance than the theoretical limit due to imperfections in the 2D structure, such as grain boundaries, lattice defects, and oxidative traps. Graphene produced by scalable production methods, such as chemical vapor deposition (CVD) and epitaxial growth, usually has a sheet resistance of hundreds of Ω/sq at around 80% transmission for the 550 nm wavelength.[13] Graphene has high sheet resistance because its intrinsic carrier concentration is low. The intrinsic carrier concentration is only about 9×10^{10} cm^{-2} at room temperature (or 300 K)[14] or about 10^{11} to 10^{12} cm^{-2} with unintentional or surface adsorbate doping.[15] Theoretical calculations have suggested that higher values of $\sigma_{dc}/\sigma_{op} = 330$ or $R_s = 11$ Ω/sq

* Address correspondence to pleu@pitt.edu.

Received for review February 25, 2015 and accepted April 29, 2015.

Published online April 29, 2015
10.1021/acsnano.5b01243

at $T = 90\%$ may be achievable by doping.[12] However, highly doped graphene still falls short of typical industry needs of $\sigma_{dc}/\sigma_{op} = 350$ or $R_s = 10\ \Omega$/sq at $T = 90\%$.[12]

In this paper, we demonstrate that single-layered graphene may be integrated with microscale metal grids to form hierarchical graphene/metal grid structures that have significantly improved performance over graphene thin films or metal grid structures by themselves. The hierarchical structure exhibits σ_{dc}/σ_{op} as high as 8900 and 94% diffusive transmission at 0.6 Ω/sq. In contrast, the single layer of graphene has $\sigma_{dc}/\sigma_{op} = 12$ and 97% diffusive transmission at 1000 Ω/sq. The sheet resistance may be decreased by over 3 orders of magnitude with only a slight decrease in transmission. The hierarchical structures demonstrate uniform conductivity over large areas and local current conductivity due to the graphene. The fabrication process, consisting of graphene deposition and transfer and metal photolithography patterning, has the potential for scalable manufacturing. Thermal and bending tests also demonstrate the improved sheet resistance of the hierarchical structures compared to microscale metal grids as the graphene limits oxidation and enhances the adhesion of the metal to the substrate.

RESULTS AND DISCUSSION

Figure 1a shows a schematic of the hierarchical graphene/metal grid structure. The graphene is produced on copper foils by CVD[16] and transferred onto a hexagonal microscale silver (Ag) grid using poly(methyl methacrylate) (PMMA). The microscale Ag grids are fabricated using photolithography and e-beam evaporation. The morphology of the microscale grid is defined by the pitch of the hexagonal array a and the width w and thickness t of the metal. Please see the Supporting Information for details about the fabrication process. The microscale metal grids by themselves may exhibit over 90% transmission at less than 0.5 Ω/sq sheet resistance.[17,18] However, they are not a good transparent conductor material *per se* because the distance between the metal is hundreds of microns, and this results in the poor local collection or delivery of carriers. Figure 1b shows a representative scanning electron microscope (SEM) image of the hierarchical structure fabricated on a quartz substrate. For this particular sample, $a = 300\ \mu$m, $w = 10\ \mu$m, and $t = 1\ \mu$m. The SEM image is taken at the edge of the deposited graphene sheet. There is no graphene in the top left of the SEM image; the bright contrast in this area is a result of surface charging due to poor conductivity in the empty areas between the microscale Ag grids. The lower right of the SEM image is covered by graphene and therefore shows a much darker contrast. The graphene sheet can cover the microscale Ag grids conformally without significant cracks and wrinkles. The hierarchical graphene/Ag grid samples exhibit a uniformly transparent appearance over an area of about 2 cm × 2 cm, as shown in Figure 1c. Conductive atomic force microscopy measurements demonstrate that the hierarchical structures exhibit uniform localized current conductivity (Figure S1) at the microscale. This is in contrast to random networks of carbon nanotubes or nanowires. The high uniformity of localized current conductivity for the hierarchical structures is desirable

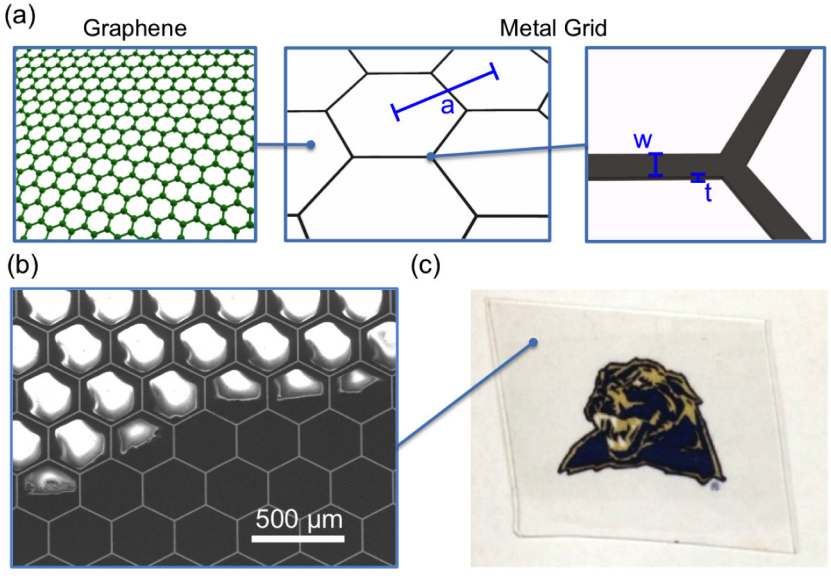

Figure 1. (a) Schematic of the hierarchical graphene/metal grid transparent conductor, where the structure consists of a single-layer graphene sheet fabricated by CVD and transferred on a hexagonal metal grid with pitch *a*, grid width *w*, and thickness *t*. (b) SEM image for the edge of a graphene sheet on a microscale silver grid with $a = 300\ \mu$m, $w = 10\ \mu$m, and $t = 1\ \mu$m on a rigid quartz substrate. The dark part on the bottom is where there is a graphene sheet. (c) Optical image of graphene/microscale Ag grid on the quartz substrate (permission for the use of the logo was obtained from the University of Pittsburgh).

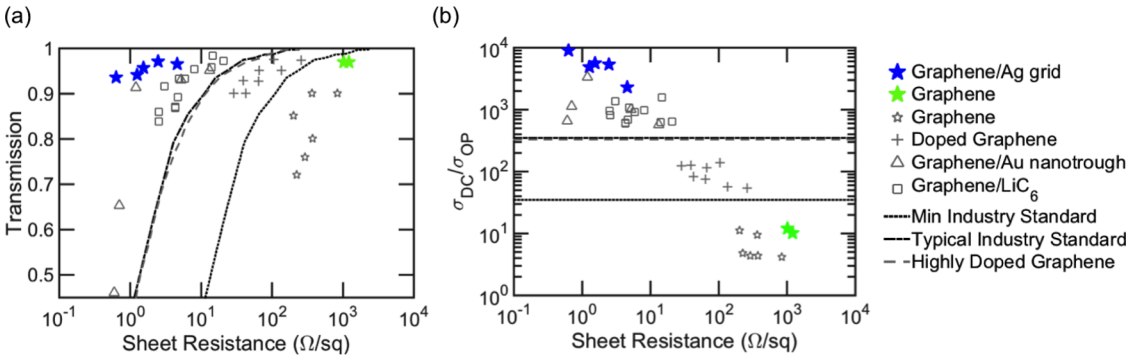

Figure 2. (a) Transmission *versus* sheet resistance for graphene in the literature. The minimum industry standard, typical industry standard, and theoretical calculation of highly doped graphene are plotted with lines.[19] Experimental data for CVD graphene,[1320−24] roll-to-roll synthesized and transferred doped graphene (R2R),[9] graphene with gold nanotroughs,[25] and lithiated graphene[26] are also shown. (b) Figure of merit of the various graphene components compared with the minimum industry standard and theoretical estimates of the doped graphene limit.

for a more uniform appearance in flat panel displays and better carrier collecting ability in solar cells.

Figure 2a plots the relationship between the diffusive transmission and sheet resistance for a variety of graphene thin films. Our experimental data for the hierarchical graphene/Ag grid structures are plotted with blue stars. The diffusive and specular transmission of the samples were measured using a spectrophotometer with and without an integrating sphere, respectively. The diffusive transmission accounts for transmission from all angles, while the specular transmission only accounts for normal transmission. Our diffusive transmission data are plotted at the λ = 550 nm wavelength, which is near the middle of the visible spectrum. The effect of the substrate has been excluded by renormalization. The performance of the graphene without the Ag grids is shown with green stars. The sheet resistance of the hierarchical structures slightly increased from that of the metal grid due to some oxidation or corrosion of the metal during the graphene transfer. For example, our Ag grid with $a = 200\ \mu$m, $w = 5\ \mu$m, and $t = 1\ \mu$m exhibited R_s = 0.5 Ω/sq and diffusive transmission of 98%. After graphene transfer, the sheet resistance increased to R_s = 1.2 Ω/sq and diffusive transmission dropped to 94%.

The minimum and typical transparent conductor requirements are shown with the black dotted and dash-dotted lines, and the theoretical limit for highly doped graphene is shown with the gray dashed line. For comparison purposes, we plot the best graphene data that we are aware of in the literature for CVD intrinsic graphene[13,20−24] and roll-to-roll synthesized and transferred doped graphene[9] using gray markers. Other graphene films have also been reported, such as exfoliated graphene,[27] reduced graphene oxide,[28,29] and chemically modified graphene,[30] though these tend to have much worse performance with sheet resistances over 1000 Ω/sq. Two structures, graphene with Au nanotroughs[25] and lithiated graphene,[26] have recently demonstrated performances above theoretical limit estimates for doped graphene and are also plotted. Our CVD single layer of graphene exhibits very high transmission of 97%, but the sheet resistance is also very high and over 1000 Ω/sq. If we integrate the graphene with the Ag microscale grids, the sheet resistance may be decreased substantially to between 0.6 and 5 Ω/sq. The transmission decreases only slightly to between 94 and 97%.

Figure 2b plots the FoM σ_{dc}/σ_{op} of these transparent conductors *versus* sheet resistance. σ_{dc}/σ_{op} is a commonly used FoM for transparent conductors,[31] where σ_{dc} is the dc conductivity of the material and σ_{op} is the optical conductivity. This FoM can be represented in terms of T and R_s by

$$T = \left(1+\frac{Z_0}{2R_s}\frac{\sigma_{op}}{\sigma_{dc}}\right)^{-2}$$

where $Z_0 = 377\ \Omega$ is the free space impedance. The FoM for the single-layer graphene is just slightly above 10. The hierarchical structures have significant performance with FoMs from 2300 to 8900. These FoMs are above the theoretically doped graphene limits and the highest values in the literature we are aware of for graphene-based structures.

The diffusive transmission spectra for the graphene/Ag grid structures and graphene films on quartz are plotted in Figure 3a. The geometry for the Ag grid in the hierarchical structures is $a = 200\ \mu$m, $w = 5\ \mu$m, and $t = 1\ \mu$m. The average diffusive transmission across the visible spectrum for the graphene sample is 96.8% and is 92.5% for the graphene/Ag grid sample. The incorporation of microscale Ag grids results in about a 4% drop in the average diffusive transmission of graphene in the range of 400 to 700 nm. Unlike sputtered ITO thin films, which have lower transmission in the long wavelength range,[32] the transmission spectrum for our hierarchical graphene/Ag grid is almost flat, which is important for applications such as thin film or organic solar cells. No significant plasmonic effect is observed

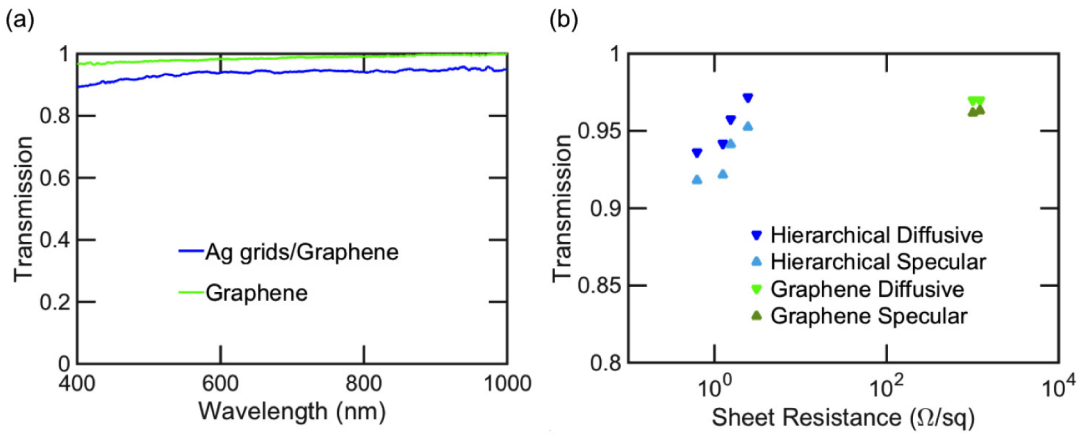

Figure 3. (a) Diffusive transmission spectrum for hierarchical graphene/Ag grid and single-layer graphene on quartz. The sheet resistance is 0.63 Ω/sq for the graphene/Ag grid sample and 1.0 kΩ/sq for the graphene sample. (b) Diffusive and specular transmission (at λ = 550 nm) for the graphene/Ag grid and graphene samples as a function of sheet resistance. The effect of substrate has been excluded.

in the transmission spectrum because the dimensions of the Ag features exceed the wavelength of interest. The samples have a uniform, transparent appearance without Moire fringes. Figure 3b demonstrates the diffusive transmission and specular transmission spectra for the hierarchical samples and the graphene control sample at λ = 550 nm. The hierarchical structures exhibit little scattering of light and very low haziness. The difference between the diffusive and specular transmission is 1.5% on average. In contrast, random Ag NW films have demonstrated a difference of about 10%.[33] The low scattering and low haziness of the graphene/Ag grid structures is beneficial for showing clear images and text in displays.

To evaluate the thermal stability of the hierarchical structures, samples were heated at 300 °C on a hot plate and compared to control samples, which only have the microscale Ag grids on quartz. Two contacts were deposited onto the samples, and the resistances of both sample were monitored. The geometry of the Ag grids in both samples is t = 0.6 μm, a = 200 μm, and w = 10 μm. Figure 4 shows the change in resistance of the hierarchical structure and control sample on the quartz substrate with the heating test. After 65 h of heating, the resistance for the sample with only microscale Ag grids increased by 83%. Oxidation-incurred conductivity degradation has been previously reported in Ag nanowire thin films after 1 h of heating in the ambient conditions at 200 °C.[34] However, the resistance of the graphene/Ag grid structures only increased by 11%. Graphene is known for its ability to block gas molecules[35] and, thus, may limit the Ag oxidation and maintain a more stable performance at elevated temperature. The resistance for both samples became constant after additional heating past 42 h. The graphene should offer additional benefits for copper nanostructures, which are more prone to oxidation than silver.[36,37]

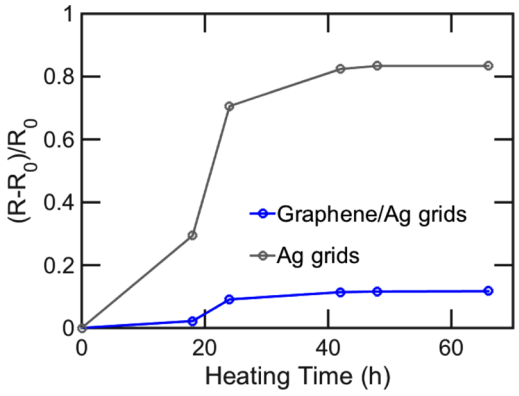

Figure 4. Heating test results for microscale Ag grids and microscale Ag grid/graphene samples at 300 °C.

To evaluate the durability of the graphene/Ag structures for flexible optoelectronics, bending tests were performed. Graphene/Ag grid and Ag grid only samples with 100 nm, 500 nm, and 1 μm Ag thicknesses were fabricated on flexible polyethylene terephthalate (PET) substrates. The Ag grids in the tests have a pitch of a = 500 μm and a width of w = 10 μm. The resistance between two deposited contacts was monitored in the bending test. The samples were bent around a steel rod with 1 cm diameter. Both compression and tension were applied by bending the Ag grid side toward the steel rod and away from the steel rod, respectively. Figure 5a,c shows the variation in the resistance of graphene/Ag grid and Ag grid on PET substrates, respectively, after both bending in compression and tension for various metal thicknesses. The 1 μm thick Ag grid (without graphene) data are not shown in Figure 5c because the Ag grid detached from the substrate after less than 10 bending cycles. The resistance for both graphene/Ag grid and Ag grid increase after bending, and the resistance increases faster for a thicker Ag grid due to greater strain on the surface of the Ag grid. A single-layer graphene sheet will protect

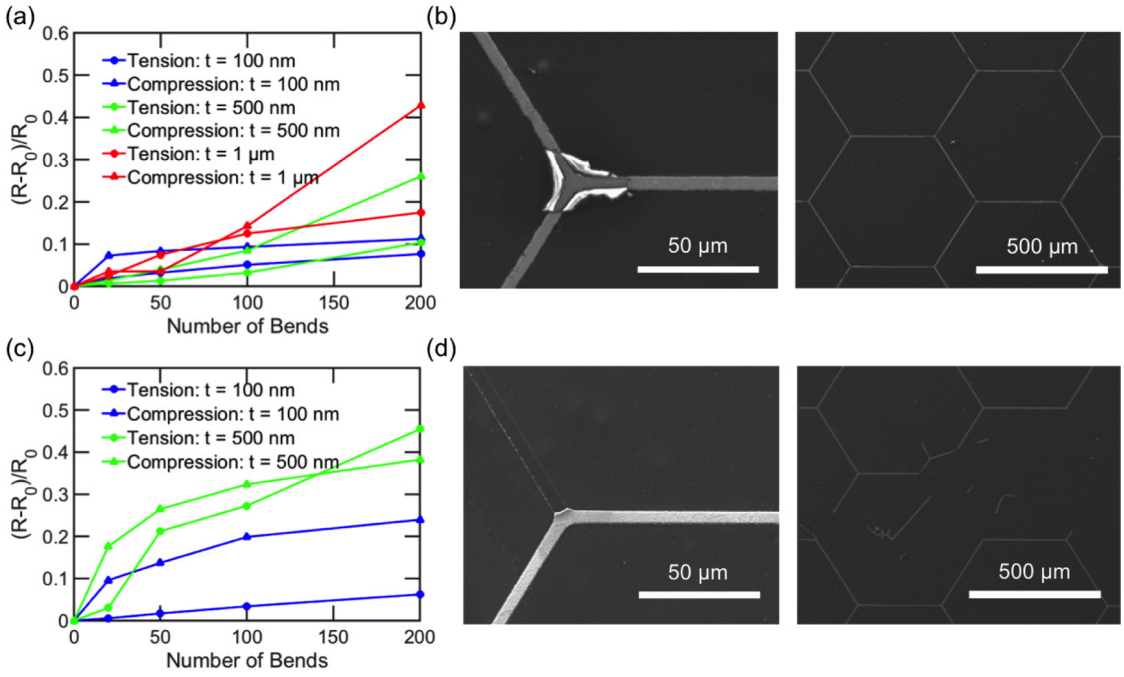

Figure 5. (a) Change in resistance *versus* number of bends for graphene/Ag grid. (b) SEM images after 200 tension bending cycles for the graphene/Ag grid. (c) Change in resistance *versus* number of bends for the Ag grid. (d) SEM images after 200 tension bending cycles for the Ag grid. The structures were fabricated on PET film. The bending curvature is 0.5 cm. The Ag grid is defined by a = 500 μm and w = 10 μm; t = 500 nm for the grids shown in (b) and (d).

the Ag grid from bending, especially for thick Ag grids. For 100 nm thick Ag grids, the resistance increased by 15.1% without graphene and by 9.5% with graphene after 200 tension bending cycles. For 500 nm thick Ag grids, the resistance increased by 41.8% without graphene and by 18.2% with graphene after 200 tension bending cycles. Figure 5b,d shows structures with metal thickness of t = 500 nm after 200 tension bending cycles. As can be seen in Figure 5b, the hierarchical structures exhibit increased resistance to cracking and delamination of the metal grids. There is some metal cracking near the vertices of the hexagons. The structures are mostly intact as the graphene strengthens the attachment between the Ag grid and PET. In contrast, as shown in Figure 5d, the Ag grids without graphene exhibit large-scale cracking and delamination.

CONCLUSIONS

In summary, a proof-of-concept graphene/microscale Ag grid transparent conductor was designed to break the limitation on transmission and resistance of graphene. The transparent conductor was fabricated on quartz and characterized. Our structures exhibit up to 94% diffusive transmission at 0.6 Ω/sq, which surpasses the theoretical performance limit of highly doped graphene thin films. The transparent conductor is stable in ambient air for prolonged heating at 300 °C due to the oxygen-blocking property of graphene. A single-layer graphene will also enhance the adhesion of the metal to the substrate for flexible optoelectronic applications, as demonstrated by bending tests. In the future, the work can be extended to the scalable manufacturing of these structures on flexible plastic substrates for flexible optoelectronic devices.

METHODS

Microscale Ag Grid Fabrication. Microscale Ag grids were fabricated using lift-off metal patterning. A layer of LOR 5B from MicroChem resist was coated onto a 0.5 mm thick quartz substrate by spin-coating, followed by a soft-bake on a hot plate at 150 °C for 5 min. A 2 μm thick photoresist AZ 4210 from AZ was then spin-coated onto the sample, followed by a soft-bake at 120 °C for 2 min. The photoresist was exposed and developed in diluted AZ 400 K from AZ for 15 s. A thin layer of titanium was first deposited as an adhesion layer onto the patterned photoresist with an e-beam evaporator, followed by Ag deposition using the same evaporator. Then, the photoresist was removed using Shipley 1165 developer remover at room temperature with gentle ultrasonication.

Graphene Synthesis. Graphene was synthesized by CVD. Cu foil (Alfa Aesar, 25 μm thick, purity of 99.8%) was cut into small strips (1.5 cm × 3 cm), rinsed with 1% diluted HCl, and placed at the center of a 1 in. diameter fused quartz tube. The furnace tube was evacuated and heated to 1000 °C under a 2.0 sccm H_2 gas flow with a pressure of 100−110 mTorr. After being annealed in H_2 atmosphere for 30 min, a CH_4 (carbon source) gas flow was also introduced into the system at a speed of 20 sccm at 1000 °C for another 30 min. Then the Cu foil was cooled to room temperature under H_2 and CH_4 gas flow (500 mTorr) and taken out of the furnace.

Graphene Transfer. The transfer process began with a spin-depositing PMMA (Aldrich, M_w 996 000) layer on one side of the Cu/graphene surface. Then the PMMA/graphene layer was separated from the Cu foil by etching in 1 M aqueous $FeCl_3$ (Sigma-Aldrich, 97%)/3.5 M HCl (Fisher Scientific, 37.1%) for 20 min. After the Cu foil was completely etched, the PMMA/graphene film was transferred to a DI water bath for cleaning and then carefully collected onto substrate and dried with a nitrogen gun. The PMMA film on the substrate was dissolved in acetone for 8 h, followed by a dichloromethane bath for another 8 h to further remove the surface PMMA residue.

Conductive Atomic Force Microscopy. Conductive atomic force microscopy was conducted using a Pt/Ir-coated probe under contact mode with a 3.0 mV sample bias. For better imaging, Au/Ti contact pads were deposited onto the sample using an e-beam evaporator before being annealed in Ar/H_2 atmosphere at 400 °C for 2 h. The current maps were obtained as well as the height maps.

Conflict of Interest: The authors declare no competing financial interest.

Acknowledgment. This work was supported in part by NSF Grant Nos. 1233151 and 1235979. The authors would also like to thank the Mascaro Center for Sustainable Innovation for support.

Supporting Information Available: Details of the design of the hierarchical grids; fabrication process; and conductive atomic force microscope studies. The Supporting Information is available free of charge on the ACS Publications website at DOI: 10.1021/acsnano.5b01243.

REFERENCES AND NOTES

1. Granqvist, C. G.; Hultåker, A. Transparent and Conducting ITO Films: New Developments and Applications. *Thin Solid Films* **2002**, *411*, 1–5.
2. Minami, T. Present Status of Transparent Conducting Oxide Thin-Film Development for Indium-Tin-Oxide (ITO) Substitutes. *Thin Solid Films* **2008**, *516*, 5822–5828.
3. Lewis, B. G.; Paine, D. C. Applications and Processing of Transparent Conducting Oxides. *MRS Bull.* **2000**, *25*, 22–27.
4. Barnes, T. M.; Wu, X.; Zhou, J.; Duda, A.; van de Lagemaat, J.; Coutts, T. J.; Weeks, C. L.; Britz, D. A.; Glatkowski, P. Single-Wall Carbon Nanotube Networks as a Transparent Back Contact in CdTe Solar Cells. *Appl. Phys. Lett.* **2007**, *90*, 243503.
5. Cao, Q.; Zhu, Z.; Lemaitre, M. G.; Xia, M.; Shim, M.; Rogers, J. A. Transparent Flexible Organic Thin-Film Transistors That Use Printed Single-Walled Carbon Nanotube Electrodes. *Appl. Phys. Lett.* **2006**, *88*, 113511.
6. Dan, B.; Irvin, G. C.; Pasquali, M. Continuous and Scalable Fabrication of Transparent Conducting Carbon Nanotube Films. *ACS Nano* **2009**, *3*, 835–843.
7. Southard, A.; Sangwan, V.; Cheng, J.; Williams, E. D.; Fuhrer, M. S. Solution-Processed Single Walled Carbon Nanotube Electrodes for Organic Thin-Film Transistors. *Org. Electron.* **2009**, *10*, 1556–1561.
8. Tien, H.; Huang, Y.; Yang, S.; Wang, J.; Ma, C. M. The Production of Graphene Nanosheets Decorated with Silver Nanoparticles for Use in Transparent, Conductive Films. *Carbon* **2011**, *49*, 1550–1560.
9. Bae, S.; Kim, H.; Lee, Y.; Xu, X.; Park, J.; Zheng, Y.; Balakrishnan, J.; Lei, T.; Kim, H. R.; Song, Y. I.; et al. Roll-to-Roll Production of 30-in. Graphene Films for Transparent Electrodes. *Nat. Nanotechnol.* **2010**, *5*, 574–578.
10. Wu, J.; Becerril, H. A.; Bao, Z.; Liu, Z.; Chen, Y.; Peumans, P. Organic Solar Cells with Solution-Processed Graphene Transparent Electrodes. *Appl. Phys. Lett.* **2008**, *92*, 263302.
11. Eda, G.; Lin, Y.-Y.; Miller, S.; Chen, C.-W.; Su, W.-F.; Chhowalla, M. Transparent and Conducting Electrodes for Organic Electronics from Reduced Graphene Oxide. *Appl. Phys. Lett.* **2008**, *92*, 233305.
12. De, S.; Coleman, J. N. Are There Fundamental Limitations on the Sheet Resistance and Transmittance of Thin Graphene Films? *ACS Nano* **2010**, *4*, 2713–2720.
13. Kim, K. S.; Zhao, Y.; Jang, H.; Lee, S. Y.; Kim, J. M.; Kim, K. S.; Ahn, J.-H.; Kim, P.; Choi, J.-Y.; Hong, B. H. Large-Scale Pattern Growth of Graphene Films for Stretchable Transparent Electrodes. *Nature* **2009**, *457*, 706–710.
14. Fang, T.; Konar, A.; Xing, H.; Jena, D. Carrier Statistics and Quantum Capacitance of Graphene Sheets and Ribbons. *Appl. Phys. Lett.* **2007**, *91*, 092109.
15. Yin, Y.; Cheng, Z.; Wang, L.; Jin, K.; Wang, W. Graphene, a Material for High Temperature Devices—Intrinsic Carrier Density, Carrier Drift Velocity, and Lattice Energy. *Sci. Rep.* **2014**, *4*, 5758.
16. Li, X.; Cai, W.; An, J.; Kim, S.; Nah, J.; Yang, D.; Piner, R.; Velamakanni, A.; Jung, I.; Tutuc, E.; et al. Large-Area Synthesis of High-Quality and Uniform Graphene Films on Copper Foils. *Science* **2009**, *324*, 1312–1314.
17. Gao, T.; Leu, P. W. The Role of Propagating Modes in Silver Nanowire Arrays for Transparent Electrodes. *Opt. Express* **2013**, *21*, A419–A429.
18. Gao, T.; Leu, P. W. Copper Nanowire Arrays for Transparent Electrodes. *J. Appl. Phys.* **2013**, *114*, 063107.
19. De, S.; King, P. J.; Lotya, M.; O'Neill, A.; Doherty, E. M.; Hernandez, Y.; Duesberg, G. S.; Coleman, J. N. Flexible, Transparent, Conducting Films of Randomly Stacked Graphene from Surfactant-Stabilized, Oxide-Free Graphene Dispersions. *Small* **2010**, *6*, 458–464.
20. Cai, W.; Zhu, Y.; Li, X.; Piner, R. D.; Ruoff, R. S. Large Area Few-Layer Graphene/Graphite Films as Transparent Thin Conducting Electrodes. *Appl. Phys. Lett.* **2009**, *95*, 123115.
21. Li, X.; Zhu, Y.; Cai, W.; Borysiak, M.; Han, B.; Chen, D.; Piner, R. D.; Colombo, L.; Ruoff, R. S. Transfer of Large-Area Graphene Films for High-Performance Transparent Conductive Electrodes. *Nano Lett.* **2009**, *9*, 4359–4363.
22. Wang, Y.; Chen, X.; Zhong, Y.; Zhu, F.; Loh, K. P. Large Area, Continuous, Few-Layered Graphene as Anodes in Organic Photovoltaic Devices. *Appl. Phys. Lett.* **2009**, *95*, 063302.
23. Reina, A.; Jia, X.; Ho, J.; Nezich, D.; Son, H.; Bulovic, V.; Dresselhaus, M. S.; Kong, J. Large Area, Few-Layer Graphene Films on Arbitrary Substrates by Chemical Vapor Deposition. *Nano Lett.* **2009**, *9*, 30–35.
24. Güneş, F.; Han, G. H.; Kim, K. K.; Kim, E. S.; Chae, S. J.; Park, M. H.; Jeong, H.-K.; Lim, S. C.; Lee, Y. H. Large-Area Graphene-Based Flexible Transparent Conducting Films. *Nano* **2009**, *4*, 83–90.
25. An, B. W.; Hyun, B. G.; Kim, S.-Y.; Kim, M.; Lee, M.-S.; Lee, K.; Koo, J. B.; Chu, H. Y.; Bae, B.-S.; Park, J.-U. Stretchable and Transparent Electrodes Using Hybrid Structures of Graphene-Metal Nanotrough Networks with High Performances and Ultimate Uniformity. *Nano Lett.* **2014**, *14*, 6322–6328.
26. Bao, W.; Wan, J.; Han, X.; Cai, X.; Zhu, H.; Kim, D.; Ma, D.; Xu, Y.; Munday, J. N.; Drew, H. D.; et al. Approaching the Limits of Transparency and Conductivity in Graphitic Materials through Lithium Intercalation. *Nat. Commun.* **2014**, *5*, 4224.
27. Biswas, S.; Drzal, L. T. A Novel Approach To Create a Highly Ordered Monolayer Film of Graphene Nanosheets at the Liquid−Liquid Interface. *Nano Lett.* **2009**, *9*, 167–172.
28. Wang, X.; Zhi, L.; Mullen, K. Transparent, Conductive Graphene Electrodes for Dye-Sensitized Solar Cells. *Nano Lett.* **2008**, *8*, 323–327.
29. Liang, Y.; Frisch, J.; Zhi, L.; Norouzi-Arasi, H.; Feng, X.; Rabe, J. P.; Koch, N.; Müllen, K. Transparent, Highly Conductive Graphene Electrodes from Acetylene-Assisted Thermolysis of Graphite Oxide Sheets and Nanographene Molecules. *Nanotechnology* **2009**, *20*, 434007.
30. Zhu, Y.; Cai, W.; Piner, R. D.; Velamakanni, A.; Ruoff, R. S. Transparent Self-Assembled Films of Reduced Graphene Oxide Platelets. *Appl. Phys. Lett.* **2009**, *95*, 103104.
31. Dressel, M.; Grüner, G. *Electrodynamics of Solids: Optical Properties of Electrons Matter*, 1st ed.; Cambridge University Press: Cambridge, UK, 2002.
32. Yang, L.; Zhang, T.; Zhou, H.; Price, S. C.; Wiley, B. J.; You, W. Solution-Processed Flexible Polymer Solar Cells with Silver

Nanowire Electrodes. *ACS Appl. Mater. Interfaces* **2011**, *3*, 4075–4084.
33. Hu, L.; Kim, H. S.; Lee, J.; Peumans, P.; Cui, Y. Scalable Coating and Properties of Transparent, Flexible, Silver Nanowire Electrodes. *ACS Nano* **2010**, *4*, 2955–2963.
34. Lee, J.; Connor, S. T.; Cui, Y.; Peumans, P. Solution-Processed Metal Nanowire Mesh Transparent Electrodes. *Nano Lett.* **2008**, *8*, 689–692.
35. Chen, S.; Brown, L.; Levendorf, M.; Cai, W.; Ju, S.-Y.; Edgeworth, J.; Li, X.; Magnuson, C. W.; Velamakanni, A.; Piner, R. D.; et al. Oxidation Resistance of Graphene-Coated Cu and Cu/Ni Alloy. *ACS Nano* **2011**, *5*, 1321–1327.
36. Gao, T.; Wang, B.; Ding, B.; Lee, J.-K.; Leu, P. W. Uniform and Ordered Copper Nanomeshes by Microsphere Lithography for Transparent Electrodes. *Nano Lett.* **2014**, *14*, 2105–2110.
37. Chang, Y.; Lye, M. L.; Zeng, H. C. Large-Scale Synthesis of High-Quality Ultralong Copper Nanowires. *Langmuir* **2005**, *21*, 3746–3748.